

## INFLUENCE OF NUCLEAR SYMMETRY ENERGY ON PROPERTIES OF NEUTRON STAR OUTER CORE MATTER

*Jun-Jie Guo & Wei Chen*

*Research Scholar, Department of Physics, Jinan University, Guangzhou, China*

### ABSTRACT

Based on the mean-field approximation of relativistic  $\sigma$ - $\omega$ - $\rho$  model with the nonlinear self-interaction of  $\sigma$  meson and density-dependent coupling constants respectively, the nuclear symmetry energy  $S$ , its slope  $L$  and curvature  $K$  as well as the proton fraction  $x_p$  and the pressure  $P$  of the matter in the outer core of neutron star are studied. It is found that greater  $S$  in high-density region and  $L$  at saturation density produce greater proton fraction and pressure of neutron star outer core matter. And the density threshold of proton super fluidity and the direct URCA process, which are model dependent, decrease as the nuclear symmetry energy increases.

**KEYWORDS:** Nuclear Symmetry Energy, Pressure, Proton Fraction, Neutron Star Outer Core Matter

### Article History

**Received: 17 Mar 2019 | Revised: 28 Mar 2019 | Accepted: 10 Mar 2019**

**PACS:** 21.65.Ef, 26.60.Kp, 26.60.Dd

### INTRODUCTION

$S(\rho_B)$  is defined as the nuclear symmetry energy (NSE) if the energy per particle of nuclear matter is expanded as the following series[1, 2]:

$$E(\rho_B, \alpha) = E(\rho_B, 0) + S(\rho_B) \cdot \alpha^2 + S_4(\rho_B) \cdot \alpha^4 + \dots (1)$$

It means the impact of isospin asymmetry  $\alpha = (\rho_n - \rho_p) / \rho_B$  on energy per particle of nuclear matter and reflects the difficulties of nuclear matter from symmetry to asymmetry.  $\rho_B = \rho_n + \rho_p$  with  $\rho_n$ ,  $\rho_p$  and  $\rho_B$  to be the densities of neutron, proton, and nucleon, respectively.

NSE has been studied extensively in many experiments [3], among which the more prominent are the measurement of nuclear polarizability[4] and nuclear mass[5], parity violation in electro scattering on nuclei[6], the giant dipole resonances[7], heavy ion collisions[8-10] and nucleon optical potential[11], direct detection of gravitational waves[12], X-ray observations of neutron stars[13, 14] etc. The theoretical works of NSE mainly include the research of finite nuclei and infinite nuclear matter [15-25]. The NSE  $J \approx 32$  MeV[3, 5] at saturation density and the binding energy of infinite symmetric nuclear matter is roughly equal to 16 MeV with incompressibility coefficient  $K_0 = 240 \pm 20$  MeV here[26].

There are two kinds of results of Hartree-Fock approximation of asymmetric nuclear matter according to the density-dependence of NSE around saturation density [19, 27-31]. Neutron skin of neutron-rich nucleus is sensitive to NSE under saturation density [32-36]. To highlight this dependence, the neutron skin has been widely studied by potential

theory and field theory [21, 37-40]. Similarly, the NSE has an important influence on the properties of a neutron star of which the outer core matter consisted mainly of neutrons, protons, electrons, and muons can be simulated by homogeneous infinite nuclear matter above saturation density [41-43]. The fraction of particles in a neutron star, and therefore, the equation of state (EOS) of neutron star matter are affected by NSE [43-50]. EOS is a key input when we study the properties of neutron stars, so the radius of a neutron star [51, 52], tidal deformation [53-55], the core-crust transition [56, 57], and other gravitational properties [58-61] are all related to NSE. And most directly, the fractions of protons  $x_p$  are constrained by NSE [62]. The  $^1S_0$  proton pairing is predicted to exist, while the neutron superfluidity may occur mainly in the coupled  $^3P_2$ - $^3F_2$  two-neutron channel in the quantum fluid in the outer core when the proton density increases to the range about  $\rho_0/10$ . The superfluidity of neutrons, protons, hyperons in the  $^1S_0$  channel and neutrons in the  $^3P_2$  channel has been studied extensively [63]. However, density range where energy gaps appear in neutron stars is still unclear. On the other hand, the direct URCA process which will be restrained by superfluidity of nucleons is allowed at  $x_p \approx 1/9$  [44, 64-66]. The competition between superfluidity of nucleons and direct URCA process plays an important role in evolution of neutron stars [67-70]. The direct URCA process is allowed in several models with appropriate density-dependence of NSE when the density is over maximum density  $0.5 \text{ fm}^{-3}$ , while it is not allowed in some other models for the density needed is greater than the density of the most massive stella core. A detailed discussion in this aspect is shown in Ref. [71].

Following these works, the impact of NSE on pressure and proton fraction in the outer core of neutron star will be studied in the relativistic  $\sigma$ - $\omega$ - $\rho$  model and the results under skyrme model will also be reproduced for comparing in this paper.

The basic theories about relativistic  $\sigma$ - $\omega$ - $\rho$  model and NSE will be introduced in the following section. And the numerical calculation results and analysis will be presented in section 3. The summary will be given in the last section.

## Formalism

The Lagrangian density in the relativistic  $\sigma$ - $\omega$ - $\rho$  model is

$$\begin{aligned} \mathcal{L} = & \sum_{B=n,p} \bar{\psi}_B \left( \gamma_\mu \left( i\partial^\mu - g_\omega V^\mu - \frac{1}{2} g_\rho \boldsymbol{\tau} \cdot \mathbf{b}^\mu \right) - (M - g_\sigma \phi) \right) \psi_B + \frac{1}{2} (\partial_\mu \phi \partial^\mu \phi - m_\sigma^2 \phi^2) - \frac{1}{4} \omega_{\mu\nu} \omega^{\mu\nu} + \\ & \frac{1}{2} m_\omega^2 V_\mu V^\mu - \frac{1}{4} \rho_{\mu\nu} \rho^{\mu\nu} + \frac{1}{2} m_\rho^2 \mathbf{b}_\mu \mathbf{b}^\mu - \frac{1}{3!} c \phi^3 - \frac{1}{4!} d \phi^4 + \sum_\lambda \bar{\psi}_\lambda (i\gamma_\mu \partial^\mu - m_\lambda) \psi_\lambda, \end{aligned} \quad (2)$$

$$\begin{aligned} \omega_{\mu\nu} &= \partial_\mu V_\nu - \partial_\nu V_\mu, \\ \rho_{\mu\nu} &= \partial_\mu \mathbf{b}_\nu - \partial_\nu \mathbf{b}_\mu, \end{aligned}$$

where  $\psi_B$ ,  $\psi_\lambda$ ,  $\phi$ ,  $V_\mu$ , and  $\mathbf{b}_\mu$  are the field operators of nucleons (neutron and proton), leptons (electron and muon),  $\sigma$ ,  $\omega$  and  $\rho$  meson, and  $M$ ,  $m_\lambda$ ,  $m_\sigma$ ,  $m_\omega$  and  $m_\rho$  their mass, respectively.  $g_\sigma$ ,  $g_\omega$ , and  $g_\rho$  are the coupling constants between nucleons and  $\sigma$ ,  $\omega$ ,  $\rho$  meson, respectively.

By the mean field approximation, we can obtain the expression of the energy density and pressure of infinite nuclear matter:

$$\begin{aligned} \mathcal{E} = & \sum_{i=n,p,e,\mu} \frac{\gamma}{(2\pi)^3} \int_{\text{d}^3k} d^3k \sqrt{k^2 + m_i^{*2}} + \frac{1}{2} (m_\omega^2 V_0^2 + m_\rho^2 b_0^2 + m_\sigma^2 \phi_0^2) + \frac{1}{3!} c \phi_0^3 + \frac{1}{4!} d \phi_0^4 \\ = & \frac{\gamma}{16\pi^2} \sum_{i=n,p,e,\mu} \left( (2k_{fi}^3 + m_i^{*2} k_{fi}) E_i^* + m_i^{*4} \ln \frac{m_i^*}{k_{fi} + E_i^*} \right) + \frac{1}{2} \left( \frac{g_\omega}{m_\omega} \rho_B \right)^2 + \frac{1}{2} \left( \frac{g_\rho}{2m_\rho} \rho_B \alpha \right)^2 + \\ & \frac{1}{2} m_\sigma^2 \phi_0^2 + \frac{1}{3!} c \phi_0^3 + \frac{1}{4!} d \phi_0^4, \end{aligned} \quad (3)$$

$$\begin{aligned}
 P_B &= \frac{1}{3} \sum_{i=n,p,e,\mu} \frac{\gamma}{(2\pi)^3} \int_{k_{fi}} d^3k \frac{k^2}{\sqrt{k^2 + m_i^{*2}}} + \frac{1}{2} m_\omega^2 V_0^2 + \frac{1}{2} m_\rho^2 b_0^2 - \frac{1}{2} m_\sigma^2 \phi_0^2 - \frac{1}{3!} c \phi_0^3 - \frac{1}{4!} d \phi_0^4 \\
 &= \frac{\gamma}{16\pi^2} \sum_{i=n,p,e,\mu} \left( \left( \frac{2}{3} k_{fi}^3 - m_i^{*2} k_{fi} \right) E_i^* - m_i^{*4} \ln \frac{m_i^*}{k_{fi} + E_i^*} \right) + \frac{1}{2} \left( \frac{g_\omega}{m_\omega} \rho_B \right)^2 + \frac{1}{2} \left( \frac{g_\rho}{2m_\rho} \rho_B \alpha \right)^2 - \\
 &\quad \frac{1}{2} m_\sigma^2 \phi_0^2 - \frac{1}{3!} c \phi_0^3 - \frac{1}{4!} d \phi_0^4,
 \end{aligned} \tag{4}$$

where  $\phi_0$ ,  $V_0$  and  $b_0$  are the mean field of  $\sigma$ ,  $\omega$  and  $\rho$  meson, respectively, and the nucleon density  $\rho_B = \frac{\gamma}{6\pi^2} \sum k_{fB}^3$ ,  $E_B^* = \sqrt{k_{fB}^2 + m_B^{*2}}$  with effective nucleon mass  $m_B^* = m_B - g_\sigma \phi_0$ , and  $E_\lambda^* = \sqrt{k_{f\lambda}^2 + m_\lambda^{*2}}$  with effective lepton mass  $m_\lambda^* = m_\lambda$

The energy per nucleon is defined by

$$E(\rho_B, \alpha) = \frac{\mathcal{E}}{\rho_B}. \tag{5}$$

$$S(\rho_B) = J + L_{sym} x + \frac{1}{2} K_{sym} x^2 + \dots; \quad x = \frac{\rho_B - \rho_0}{3\rho_0}, \tag{6}$$

The NSE can be expanded as following again:

where the slope parameter  $L_{sym} = \left. \frac{\partial S}{\partial x} \right|_{x=0}$  and the curvature parameter  $K_{sym} = \left. \frac{\partial^2 S}{\partial x^2} \right|_{x=0}$ .  $L_{sym} = 58.7 \pm 28.1$  MeV[3,5],  $400 \leq K_{sym} \leq 100$  MeV[21,72].

The coupling constants are treated in two ways to reproduce the saturation properties of infinite symmetric nuclear matter. The first is called non-linear model (NL) in which  $\sigma$ ,  $\omega$ , and  $\rho$  are treated as constants and the nonlinear self-interaction of  $\sigma$  meson  $c$ ,  $d$  is introduced; and the second is called density-dependent coupling model (DDC) in which  $g_\sigma$ ,  $g_\omega$  and  $g_\rho$  are treated as density-dependent and  $c=d=0$ , and the density-dependent formulas of the coupling constants  $g_\sigma$ ,  $g_\omega$ , and  $g_\rho$  are assumed to be

$$g_\sigma = g_{\sigma 0} \cdot \frac{1 + a_\sigma (x_B + c_\sigma)^2}{1 + b_\sigma (x_B + c_\sigma)^2}, \tag{7}$$

$$g_\omega = g_{\omega 0} \cdot \frac{1 + a_\omega (x_B + c_\omega)^2}{1 + b_\omega (x_B + c_\omega)^2}, \tag{8}$$

$$g_\rho = g_{\rho 0} \cdot e^{-a_\rho (x_B - 1)}, \tag{9}$$

where  $x_B = \rho_B / \rho_0$ .

Neutrons will decay into protons in the outer core of neutron star if  $\mu_n > \mu_p + \mu_e$ , thus the chemical equilibrium condition must be considered[73]:

$$\mu_n = \mu_p + \mu_e, \tag{10}$$

$$\mu_e = \mu_\mu, \tag{11}$$

where  $\mu_i = \sqrt{k_{fi}^2 + m_i^{*2}}$ ,  $i = n, p, e, \mu$ .

Finally, the charge neutrality condition must be considered as well,

$$\rho_p = \rho_e + \rho_\mu. \quad (12)$$

## Numerical Results

In the NL model, the parameters are fitted to meet the saturation properties of infinite symmetric nuclear matter as listed in Table 1. And in the condition of outer core of neutron star, the fraction of protons  $x_p$ , the pressure  $P$ , NSE  $S$  with its slope  $L$  and curvature parameter  $K$  are studied, and the numerical results are depicted in Figure 1. The solid, dashed and dot-dashed curves correspond to the cases NL1, NL2, NL3 listed in Table 1, respectively. At a fixed  $x_B$ , especially in high-density region,  $P$  and  $x_p$  increase with  $S$  increasing. The values of  $L$  and  $K$  at saturation density ( $x_B=1$ ) are 75~100 MeV and -125~125 MeV, respectively, which are similar to previous works. We can also see that greater  $K_0$  produces greater values of the above quantities.

The solid circles in three cases represent the density threshold of proton superfluidity, which are  $x_B=1.93, 2.2, 2.49$  in NL1, NL2, NL3, respectively. It decreases with NSE increasing. The star represents the density threshold of the direct URCA process, which is  $x_B=3.95$  in NL1 and are larger than 4 in NL2 and NL3. It should be noted that  $K_0$  in NL1 and following DDC1 in which star appear has exceeded a reasonable value, so it is difficult for the direct URCA to take place in the outer core.

In the DDC model, the parameters which reproduce the saturation properties of infinite symmetric nuclear matter are listed in Table 2, and the numerical results are displayed in Figure 2. The solid, dashed and dot-dashed curves correspond to the cases DDC1, DDC2, and DDC3 listed in Table 2, respectively. The NSE and the pressure in high-density region are smaller obviously, while  $x_p$  is greater than the one in Figure 1. The relations between  $x_p$ ,  $P$  and  $S$  (or  $K_0$ ) at a fixed nucleon density are similar to Figure 1.

Comparing to Figure 1, the density threshold of proton superfluidity in DDC1, DDC2, DDC3 decrease to 1.89, 2.13 and 2.41 times  $\rho_0$ , respectively. The density threshold of the direct URCA process in DDC1 decreases to  $3.55\rho_0$ , and are still greater than  $4\rho_0$  in DDC2 and DDC3. The values of  $L$  and  $K$  at saturation density are 50~80 MeV and -130~-70 MeV, respectively.

For comparing, the results in the models of Ref. [74] are depicted in Figure 3. The solid, dashed and dot-dashed curves correspond to the cases MSL0, GSK□, and SkT1. The NSE, pressure, and  $x_p$  are the smallest comparing to Figure 2 and Figure 1. The relations between  $x_p$ ,  $P$  and  $S$  (or  $K_0$ ) at a fixed nucleon density are similar to the previous two cases. The proton superfluidity appears in greater density than in Figure 1, and the direct URCA process does in greater density than  $4\rho_0$ . The values of  $L$  and  $K$  at saturation density are 50~75 MeV and -125~125 MeV, respectively, which are very close to the results in our works.

## Summary

We have studied the influence of  $S$ ,  $L$ ,  $K$  on the fractions of proton and pressure of neutron star outer core matter by the meanfield approximation of the relativistic  $\sigma$ - $\omega$ - $\rho$  model. For comparing, we also reproduce the results in model MSL0, GSK□ and SkT1. NSE and pressure in NL, DDC, MSL0, GSK□, and SkT1 decrease in turn.  $x_p$  is the largest in the DDC model and smallest in MSL0, GSK□, and SkT1.  $L$  at the saturation density is about 75~100 MeV, 50~80 MeV, and 50~75 MeV, while  $K$  is -125~125 MeV, -130~-70 MeV and -125~125 MeV in NL, DDC, MSL0, GSK□, and SkT1. The

density threshold of proton superfluidity in SKT1, GSK, MSL0, NL and DDC model decrease in turn, while the one of the direct URCA processes is greater in NL1 than in DDC1 and are greater than  $4\rho_0$  in other models. The values of these quantities are model dependent, but the relations among them are similar in these models, that is, the greater  $S$  in high-density region and  $L$  at the saturation density, the greater  $x_p$  and  $P$ , but the smaller the density threshold of proton superfluidity and the direct URCA. In addition, we find that the larger  $K_0$ , the greater  $S$  in high-density region. And  $K_0$  has exceeded the reasonable value when the density threshold of the direct URCA is smaller than  $4\rho_0$ . Therefore, proton superfluidity may appear in the outer core, and the direct URCA is more likely to take place in the inner core of neutron star.

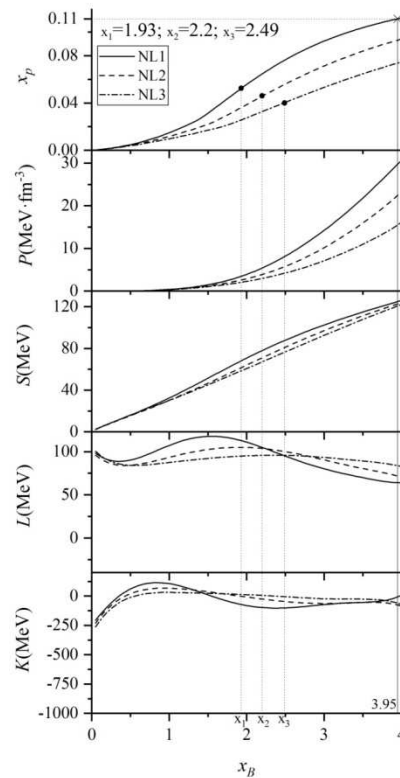


**Figure 1: The Density Dependence of the Fractions of Protons  $X_p$ , Pressure  $P$ , and NSE  $S$  as well as its Slope  $L$  and Curvature Parameter  $K$ . The Solid, Dashed and Dot-Dashed Curves Show the Results of NL1, NL2, NL3, Respectively**

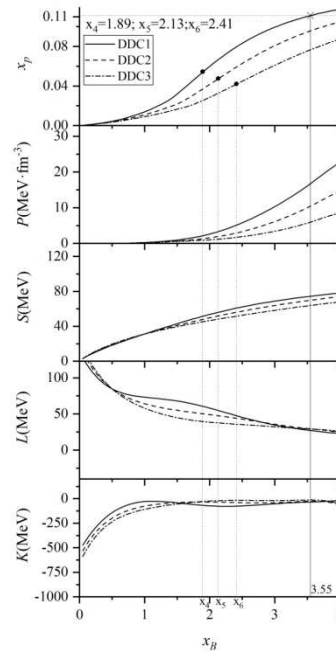


Figure 2: Similar to Figure 1 except the Parameters to be given in Table 2

Table 1: The Parameters of the Models NL1, NL2, NL3

Model	$g_{\sigma 0}$	$g_{\omega 0}$	$g_{\rho 0}$	$c$	$d$	$K_0$
NL1	10.22	13.0989	6.60	4200	-327	385.5
NL2	9.88	12.0346	6.45	8200	-715	277.7
NL3	9.31	10.6574	6.90	12500	-1100	221.4

Table 2: The Parameters of the Models DDC1, DDC2 and DDC3

Model	$g_{\sigma 0}$	$g_{\omega 0}$	$g_{\rho 0}$	$a_{\sigma}$	$b_{\sigma}$	$c_{\sigma}$	$a_{\omega}$	$b_{\omega}$	$c_{\omega}$	$a_{\rho}$	$K_0$
DDC1	8.85	11.3112	6.82	0.99	1	-0.10	1.05	1	-0.12	0.32	379.9
DDC2	8.05	9.7499	7.26	0.95	1	-0.12	1.06	1	-0.11	0.32	281.5
DDC3	7.23	8.0697	7.58	0.92	1	-0.11	1.10	1	-0.11	0.32	235.9

REFERENCES

- 1 L. W. Chen, M. K. Che, B. A. Li, *Phys. Rev. Lett*, **94**: 032701 (2005)
- 2 I. Alexandrov, A. Gerasimov et al, *Int. J. Thermophys*, **34**: 1865-1905 (2013)
- 3 M. Oertel, M. Hempel, T. Klähn, S. Typel, *Rev. Mod. Phys*, **89**: 015007 (2017)
- 4 D. Basilico, D. P. Arteaga, X. Roca-Maza, G. Colò, *Phys. Rev. C*, **92**: 035802 (2015)
- 5 B. A. Li, X. Han, *Phys. Lett. B*, **727**(1-3): 276-281 (2013)
- 6 S. Ban, C. Horowitz, R. Michaels, *J. Phys. G*, **39**: 015104 (2012)
- 7 J. M. Lattimer, A. W. Steiner, *Eur. Phys. J. A*, **50**: 40 (2014)
- 8 P. Russotto et al, *Phys. Lett. B*, **697**: 471 (2011)
- 9 P. Russotto et al, *Phys. Rev. C*, **94**: 034608 (2016)
- 10 R. Shane et al, *Nucl. Instr. Meth. A*, **784**: 513 (2015)

- 11 C. Xu, B. A. Li, L. W. Chen, *Phys. Rev. C*, **82**: 054607 (2010)
- 12 B. P. Abbott et al, *Phys. Rev. Lett*, **119**: 161101 (2017)
- 13 M. D. Trigo et al, *Astronomy & Astrophys*, **600**: A8 (2016)
- 14 T. Enoto, S. Shibata et al, *Astrophys. J. Suppl*, **231**: P8 (2017)
- 15 J. M. Lattimer, M. Prakash, *Phys. Rep*, **621**: 127-164 (2016)
- 16 N. B. Zhang, B. A. Li, *Nucl. Sci. Tech*, **29**: 178 (2018)
- 17 B. P. Abbott et al, *Phys. Rev. Lett*, **121**: 161101 (2018)
- 18 F. J. Fattoyev, W. G. Newton, B. A. Li, *Phys. Rev. C*, **90**: 022801 (2014)
- 19 B. A. Li, À. Ramos, G. Verde, I. Vidaña, I. Vidana, *Eur. Phys. J. A*, **50**: 9 (2014)
- 20 A. Carbone, G. Colò, A. Bracco, L. G. Cao, P. F. Bortignon, F. Camera, O. Wieland, *Phys. Rev. C*, **81**: 041301(R) (2010)
- 21 I. Tews, J. M. Lattimer, A. Ohnishi, E. E. Kolomeitsev, *Astrophys. J*, **848**: 105 (2017)
- 22 J. W. Holt, Y. Lim, *Phys. Lett. B*, **784**: 77-81 (2018)
- 23 R. Chen, B. J. Cai, L. W. Chen, B. A. Li, X. H. Li, C. Xu, *Phys. Rev. C*, **85**: 024305 (2012)
- 24 B. A. Li, B. J. Cai, L. W. Chen, J. Xu, *Prog. Part. Nucl. Phys*, **99**: 29-119 (2018)
- 25 Z. W. Liu, Q. Zhao, B. Y. Sun, *arXiv*: 1809.03837v1 (2018)
- 26 T. W. Li, U. Garg, Y. J. Liu et al, *Phys. Rev. Lett*, **103**: 181101 (2009)
- 27 B. A. Li, L. W. Chen, C. M. Ko, *Phys. Rep*, **464**: 113 (2008)
- 28 L. W. Chen, *Nucl. Phys. Rev*, **34**: 20 (2017)
- 29 C. J. Horowitz, E. F. Brown, Y. Kim, W. G. Lynch, R. Michaels, A. Ono, J. Piekarewicz, M. B. Tsang, H. H. Wolter, *J. Phys. G*, **41**: 093001 (2014)
- 30 M. Baldo, G. F. Burgio, *Prog. Part. Nucl. Phys*, **91**: 203 (2016)
- 31 X. Roca-maza, M. Centelles, X. Viñas, M. Warda, *Phys. Rev. Lett*, **106**: 252501 (2011)
- 32 M. Centelles, X. Roca-Maza, X. Viñas, M. Warda, *Phys. Rev. C*, **82**: 054314 (2010)
- 33 R. J. Furnstahl, *Nucl. Phys. A*, **706**: 85 (2002)
- 34 J. J. Yang, J. Piekarewicz, *Phys. Rev. C*, **97**: 014314 (2018)
- 35 S. Choi, Y. Zhang, M. K. Cheoun, Y. Kwon, K. Kim, H. C. Kim, *Phys. Rev. C*, **96**: 024311 (2017)
- 36 C. Mondal, B. K. Agrawal, M. Centelles, G. Colò, X. Roca-Maza, N. Paar, X. Viñas, S. K. Singh, S. K. Patra, *Phys. Rev. C*, **93**: 064303 (2016)
- 37 Ad. R. Raduta, F. Gulminelli, *Phys. Rev. C*, **97**: 064309 (2018)

- 38 T. Aumann, C. A. Bertulani, Schindler, S. Typel, *Phys. Rev. Lett*, **119**: 262501 (2017)
- 39 P. G. Reinhard, A. S. Umar, P. D. Stevenson, J. Piekarewicz, V. E. Oberacker, J. A. Maruhn, *Phys. Rev. C*, **93**: 044618 (2017)
- 40 A. N. Antonov, D. N. Kadrev, M. K. Gaidarov, P. Sarriguren, E. Moya de Guerra, *Phys. Rev. C*, **95**: 024314 (2017)
- 41 H. Pais, A. Sulaksono, B. K. Agrawal, C. Providência, *Phys. Rev. C*, **93**: 045802 (2016)
- 42 F. J. Fattoyev, J. Piekarewicz, C. J. Horowitz, *Phys. Rev. Lett*, **120**: 172702 (2017)
- 43 W. Weise, *Int. J. Mod. Phys*, **27**(No. 10): 1840004 (2018)
- 44 C. Providência, M. Fortin, H. Pais, A. Rabhi, *arXiv: 1811.00786v1* (2018)
- 45 X. H. Wu, A. Ohnishi, H. Shen, *Phys. Rev. C*, **98**: 065801 (2018)
- 46 X. H. Wu, H. Shen, *arXiv: 1811.06843v1* (2018)
- 47 A. W. Steiner, S. Gandolfi, *Phys. Rev. Lett*, **108**: 081102 (2011)
- 48 D. T. Loan, N. H. Tan, D. T. Khoa, J. Margueron, *Phys. Rev. C*, **83**: 065809 (2011)
- 49 S. Gandolfi, *J. Phys. Conf. Ser*, **420**: 012150 (2013)
- 50 S. Kubis, *Phys. Rev. C*, **76**: 025801 (2007)
- 51 N. Alam, B. K. Agrawal, M. Fortin, H. Pais, C. Providência, Ad. R. Raduta, A. Sulaksono, *Phys. Rev. C*, **94**: 052801(R) (2016)
- 52 S. Gandolfi, J. Carlson, S. Reddy, A. W. Steiner, R. B. Wiringa, *Eur. Phys. J. A*, **50**(2): 10 (2014)
- 53 N. B. Zhang, B. A. Li, *arXiv: 1808.07955v2* (2018)
- 54 T. Malik, N. Alam, M. Fortin, C. Providência, B. K. Agrawal, T. K. Jha, Bharat Kumar, S. K. Patra, *Phys. Rev. C*, **98**: 035804 (2018)
- 55 P. G. Krastev, B. A. Li, *arXiv: 1801.04620v1* (2018)
- 56 Z. W. Liu, Z. Qian, R. Y. Xing, J. R. Niu, B. Y. Sun, *Phys. Rev. C*, **97**: 025801 (2018)
- 57 C. O. Dorso, G. A. Frank, J. A. Lopez, *arXiv: 1807.07698v1* (2018)
- 58 N. B. Zhang, B. A. Li, *arXiv: 1809.03370v1* (2018)
- 59 D. H. Wen, B. A. Li, L. W. Chen, *Phys. Rev. Lett*, **103**: 211102 (2009)
- 60 X. T. He, F. J. Fattoyev, B. A. Li, W. G. Newton, *Phys. Rev. C*, **91**: 015810 (2015)
- 61 B. A. Li, A. W. Steiner, *Phys. Lett. B*, **642**: 436 (2006)
- 62 J. M. Lattimer, F. D. Swesty, *Nucl. Phys. A*, **535**: 331 (1991)
- 63 M. Baldo, ø. Elgarøy, L. Engvik, M. Hjorth-Jensen, H. J. Schulze, *Phys. Rev. C*, **58**: 1921 (1998b)
- 64 T. Klahn et al, *Phys. Rev. C*, **74**: 035802 (2006)



- 65 R. Cavagnoli, C. Providência, D. P. Menezes, *Phys. Rev. C*, **84**: 065810 (2011)
- 66 C. Providência et al, *Eur. Phys. J. A*, **50**: 44 (2014)
- 67 B. Friman, O. Maxwell, *Ap. J*, **232**: 541 (1979)
- 68 T. Takatsuka, R. Tamagaki, *Prog. Theor. Phys*, **97**: 345 (1997)
- 69 S. Tsuruta, *Phys. Rep*, **292**: 1 (1998)
- 70 D. Page, M. Prakash, J. M. Lattimer, A. Steiner, *Phys. Rev. Lett*, **85**: 2048 (2000)
- 71 D. Page, J. M. Lattimer, M. Prakash, A. W. Steiner, *Astrophys. J. Suppl*, **155**: 623 (2004)
- 72 N. B. Zhang, B. J. Cai, B. A. Li, W. G. Newton, J. Xu, *Nucl. Sci. Tech*, **28**: 181 (2017)
- 73 S. Nishizaki, Y. Yamamoto, T. Takatsuka, *Prog. Theor. Phys*, **105**: 607 (2001)
- 74 M. Dutra, O. Louren et al, *Phys. Rev. C*, **85**: 035201 (2012)



